A Theoretical Study of Dioxygen Activation on the Dicopper Enzyme Model

Kazunari Yoshizawa,* Takehiro Ohta, and Tokio Yamabe*

Department of Molecular Engineering, Kyoto University, Sakyo-ku, Kyoto 606-01

Institute for Fundamental Chemistry, 34-4 Takano-Nishihiraki-cho, Sakyo-ku, Kyoto 606

(Received March 10, 1997)

Dioxygen activation on the dicopper enzyme model was studied using fragment molecular orbital (FMO), Walsh-diagram, and molecular orbital overlap population (MOOP) analyses within the framework of the extended Hückel method. A dicopper peroxo model complex with a μ-η^2 : η^2-O_2 binding mode is distorted to a corresponding dioxo complex with a $Cu_2(\mu\text{-}O)_2$ diamond core along an assumed reaction coordinate describing O–O bond cleavage. FMO and Walsh-diagram analyses have clarified the bonding and orbital interactions between the dicopper active site and dioxygen. While the π_g^* orbitals of dioxygen begin with two electrons, in the early O_2 binding stages two other electrons are effectively transferred from the copper d-block orbitals to O_2. Qualitative calculations show that O–O bond cleavage should proceed with no cost of activation energy on the dicopper active site of actual enzyme systems.

The cleavage of the dioxygen O–O bond occurring on copper active sites in biological systems is one of the most important steps in the catalytic processes for dioxygen activation. Metalloenzymes having one or two copper ions in their active sites utilize the oxidizing power of O_2 for respiration and for the conversion of substrates. For example, hemocyanins are well-known oxygen carrier proteins found in mollusks and arthropods, and tyrosinase oxidizes tyrosine to form L-DOPA.[1] They have copper active sites that can bind dioxygen to lead to a peroxo species.

A dicopper enzyme, hemocyanin, shows interesting spectroscopic features in its oxidized form. For example, oxyhemocyanin exhibits an extremely intense absorption band at 350 nm with an $\varepsilon \approx 20000\ M^{-1}$ (1 M = 1 mol dm^{-3}), and a very low O–O stretching frequency of ca. 750 cm^{-1}.[2] These spectroscopic features have been proposed to be characteristic of the dimetal complex with a μ-η^2 : η^2-O_2 binding mode. From X-ray structural analyses, Kitajima and Moro-oka et al.[3] have established this type of binding mode in dicopper model complexes. Since oxytyrosinase exhibits very similar spectroscopic features, the active site of oxytyrosinase is proposed to have a dicopper core structure similar to that of oxyhemocyanin.[2h–j] The intense absorption band of these indicates that the peroxide with a μ-η^2 : η^2-O_2 mode is a very strong σ-donor ligand to two copper(II)s, while the low O–O stretching frequency is due to a weak O–O bond. According to Solomon and co-workers,[2h–j] the low O–O stretching frequency shows the peroxide to act as a π-acceptor ligand, while the π back-bonding shifts the electron density into the σ_u^* orbital (of the peroxide), which is strongly antibonding for the O–O bond. The bound dioxygen is thus activated to be cleaved.

Recently, Tolman and Que and their collaborators[4] demonstrated through a dicopper model complex similar to the active site of hemocyanin that there is an interesting equilibrium between the $[Cu_2(\mu\text{-}\eta^2 : \eta^2\text{-}O_2)]^{2+}$ and $[Cu_2(\mu\text{-}O)_2]^{2+}$ modes in solutions, as shown in Scheme 1. This equilibrium is shifted toward a μ-η^2 : η^2-O_2 core structure in dichloromethane, while it is reversely shifted toward a $(\mu\text{-}O)_2$ core structure in tetrahydrofuran. Recent ab initio calculations[5] have shown that although dicopper model complexes with μ-η^2 : η^2-O_2 and $(\mu\text{-}O)_2$ cores are very close in energy, the dioxo forms are better solvated than the peroxo forms by 5.6 to 8.4 kcal mol^{-1}. However, detailed analyses of the reaction coordinate for dioxygen cleavage on actual dicopper enzymes and model systems seem to be still lacking, concerning the reason why such a nuclear distortion induces a significant electron transfer.

From recent EXAFS and Mössbauer analyses, intermediate Q of methane monooxygenase (MMO), which can directly activate methane, is likely to have an $Fe_2(\mu\text{-}O)_2$ "diamond core" structure.[6] An O_2 evolving tetranuclear manganese cluster in photosystem II has also been proposed to consist of two $Mn_2(\mu\text{-}O)_2$ diamond core components.[7] Possible processes for the O_2 generation in this system have been investigated in terms of orbital interactions by Hoffmann et al.[8] Thus, such diamond-core structures seem to be important entities for the active sites in multinuclear metalloenzymes that use various transition metals.

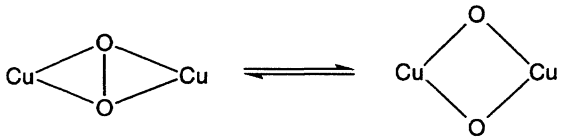

Scheme 1.

The catalytic reaction mediated by copper-based enzymes are to be initiated by important two-step reactions involving dioxygen. The first of these is an initial binding step to a dicopper active site to form a peroxo species; the second is a cleavage step of the dioxygen O–O bond. Theoretical analyses of this binding mode of dioxygen to the dicopper active site are important for a better understanding of the chemistry of hemocyanin and tyrosinase.

The μ-η^2 : η^2-O_2 binding mode mentioned above is one example for the metabolism of dicopper enzymes; there is still another possible structure. It is the μ-η^1 : η^1-O_2 mode. This binding mode was also found in dicopper model complexes by Karlin et al.[9] Moreover, such a binding mode has been crystallographically established[10—12] and theoretically analyzed[13,14] for diiron peroxo model complexes of MMO.[15] However, the naturally occurring peroxo intermediates in the dicopper enzyme system adopt the μ-η^2 : η^2-O_2 mode.

The dioxygen O–O bond cleavage performed at the active centers of metalloenzymes is an important, but unknown, step in the catalytic cycles of oxygen-activating enzymes. The purpose of this study was to understand and analyze from a qualitative point of view of orbital interactions how electron transfer occurs from the dicopper active site to dioxygen and how dioxygen cleavage proceeds from a dicopper peroxo species. We examined the reaction pathway from a dicopper model peroxo complex with the μ-η^2 : η^2-O_2 mode to a corresponding dioxo complex with the $(\mu\text{-O})_2$ mode.

Dicopper Enzyme Models

To investigate the dioxygen O–O bond cleavage on the dicopper active centers of hemocyanin and tyrosinase, we considered two theoretical model complexes, as indicated below in **1** and **2** (Chart 1). Structure **1** models a dicopper peroxo complex with a μ-η^2 : η^2-O_2 core structure. The terminal ligands of these are modeled by NH_3 because the coordination sphere of hemocyanin is composed of histidine. In these models we assumed five coordinations around each copper atom on the basis of an earlier theoretical model of Tatsumi et al.[16] We set the Cu–O(bridge) distances as 1.85 Å. The Cu–N (axial) distances were taken as 2.26 Å and those of Cu–N (equatorial) as 1.95 Å. These Cu–N bond distances have been well characterized by X-ray structural analyses using model complexes.[16] The reason why the apical Cu–N bonds are longer than the equatorial ones has been discussed in terms of orbital interactions.[16] We optimized the N(axial)–Cu–N (equatorial) and N(equatrial)–Cu–N(equatorial) angles to be 98.0° and 94.8°, respectively, with the extended Hückel method.[17] This method does not give reliable bond distances, but does model the bond angles and dihedral angles well. The O–O distances in the peroxo and dioxo forms were assumed to be 1.4 and 2.4 Å, respectively. The resultant Cu···Cu distances for **1** and **2** become 3.43 and 2.78 Å, respectively. These models belong to C_{2h} point group, the C_2 axis being on the O–O bond. Since the two coppers have charge +1 and the ligands are all neutral, the total charge of **1** and **2** is +2.

We looked at the general electronic features of **1** and **2** and analyzed the change in the electronic structure along the reaction coordinate from **1** to **2**. The levels were calculated and then filled with electrons. The extended Hückel method is not reliable for bonding energies, but models general orbital energy trends, orbital interactions, and major charge shift well. All calculations were carried out using YAeHMOP;[17] standard parameters, collected by Alvarez,[18] for copper, nitrogen, oxygen, carbon, and hydrogen are given in Table 1.

Reaction Pathway for Dioxygen Cleavage

To understand the essential orbital interactions for the bonding in a peroxo model complex **1**, we partition this complex into $Cu_2(NH_3)_6$ and O_2 fragments. Although fragment molecular orbital (FMO) analyses for this binding mode have been discussed nicely by Tatsumi and co-workers,[16] let us look at the metal-ligand interactions in detail. In Fig. 1, the molecular orbitals for $[Cu(NH_3)_3]_2(O_2)^{2+}$ are constructed by allowing two $Cu(NH_3)_3{}^{1+}$ fragments and O_2 to interact. Total ten d-block orbitals are shown in this illustration. The degenerate π_u set of O_2 (not shown in this illustration) contributes to the b_u orbitals, as can be seen from the d-block orbitals indicated in Fig. 1.

Some of the low-lying six d-block orbitals interact with dioxygen π_g^*. These will be occupied by electrons. Thus, while the π_g^* orbitals of O_2 begin in the neutral diatomic state with two electrons, two more electrons are effectively transferred from the d-block of the dimetal fragment to O_2,

Table 1. Extended Hückel Parameters

Orbital	H_{ii}(eV)	ζ_{i1}	(c_1)	ζ_{i2}	(c_2)
Cu4s	−11.4	2.2			
Cu4p	−6.06	2.2			
Cu3d	−14.0	5.95	(0.5933)	2.30	(0.5744)
O2s	−32.3	2.275			
O2p	−14.8	2.275			
C2s	−21.4	1.625			
C2p	−11.4	1.625			
N2s	−26.0	1.950			
N2p	−13.4	1.950			
H1s	−13.6	1.3			

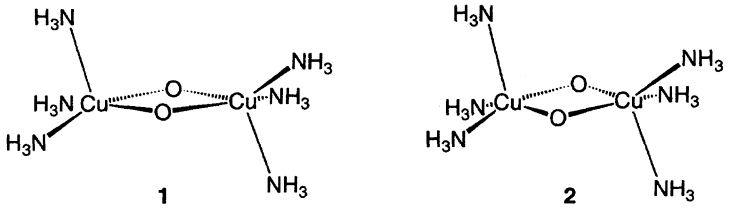

Chart 1.

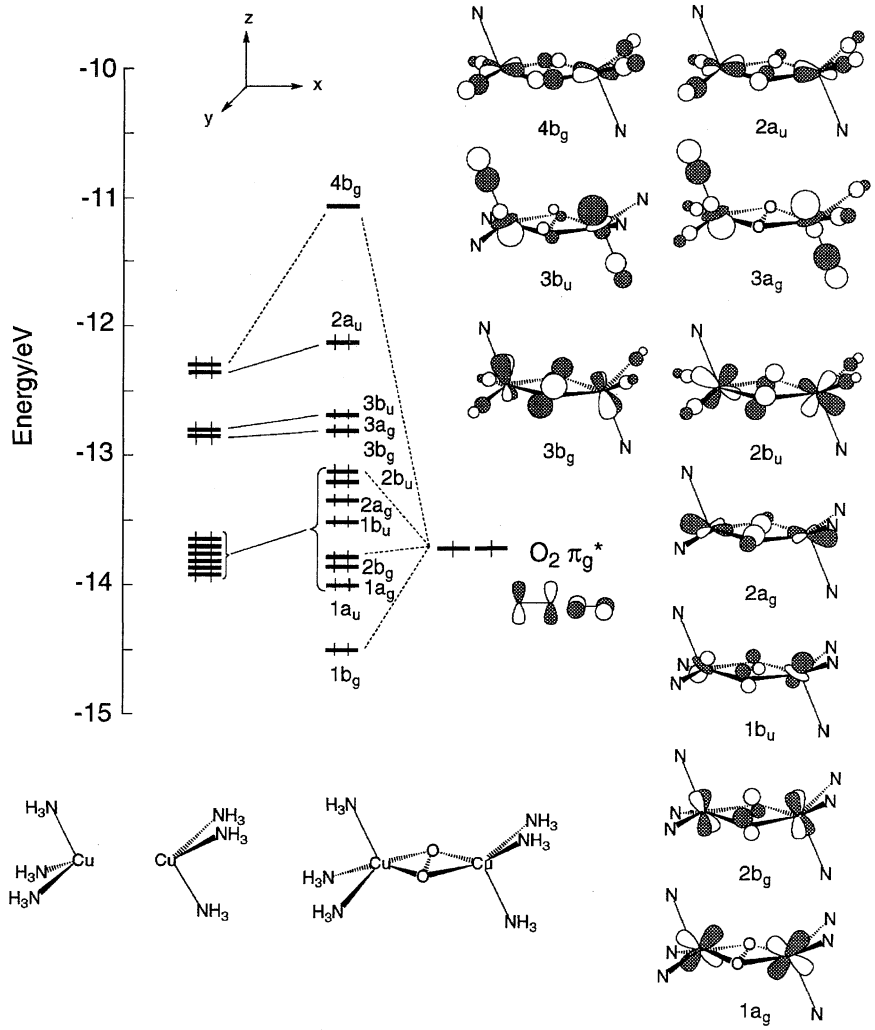

Fig. 1. Orbital interaction diagram for dicopper peroxo model complex with a μ-η^2 : η^2-O_2 core structure (**1**).

to form O_2^{2-}. The net charge of one oxygen in this peroxo model was calculated as -0.49. In this peroxo model complex, there is still one O_2 orbital that is not occupied, i.e., antibonding "σ_u^* ". The bond order, which is a measure of the net bonding, of the peroxide, is thus effectively 1. To cleave the dioxygen O–O bond completely, it is necessary to fill the antibonding "σ_u^* " orbital by two electrons.

In the next step on the catalytic cycle of the dicopper enzyme, cleavage of the peroxide O–O bond is supposed to occur through a still unknown reaction mechanism. Que and Tolman and their co-workers[4] have recently demonstrated an O–O bond cleavage using a model complex similar to oxyhemocyanin, as mentioned above. The reaction coordinate for the dioxygen cleavage can be modeled by the distortion from **1** to **2** of our theoretical models. An effective way to push the two oxygen atoms apart is to decrease the Cu–O–Cu angles, θ, as a parameter, keeping the Cu–O bond distances of 1.85 Å constant, as illustrated in **3** (Chart 2).

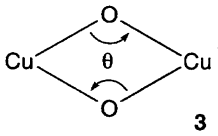

3

Chart 2.

In Fig. 2 we show a Walsh-diagram analysis along an O–O bond cleavage pathway from **1** to **2** as a function of θ defined in **3**. The related O–O distance is also given in this illustration. This distortion corresponds to an expected reaction coordinate describing the O–O bond cleavage in the dicopper model complex.[4] The dioxygen cleavage occurs with a decrease in θ in this diagram. Note that dioxygen cleavage proceeds from a peroxo species (Fig. 2 right) to a dioxo species (Fig. 2 left).

The π_g^* set (distributed into some b_g orbitals as indicated in Fig. 1) is not so dramatically changed by the distortion. For example, the $3b_g$ orbital (at -13.2 eV in Fig. 1) which is of antibonding character between dioxygen π_g^* (σ) and dicopper d_{xy}, is not remarkably changed along the reaction coordinate. Since these b_g orbitals are all occupied in this diagram, except for a high-lying one, the π_g^* set is almost fully occupied along the reaction coordinate in contrast to the σ_u^* orbital, which is not occupied in the peroxo complex, but is occupied in the dioxo one, as descried below.

When we look at the Walsh diagram from right to left, an a_u orbital goes down remarkably across the dicopper d-

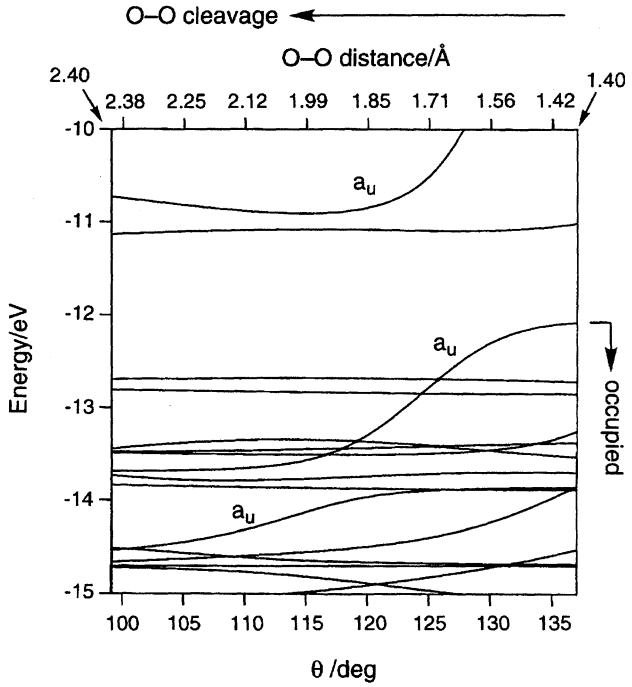

Fig. 2. Walsh diagram along an O–O bond cleavage pathway from **1** to **2** as a function of O–O distance.

block orbitals although as a consequence of the symmetry a crossing with some of these orbitals is avoided. This is the antibonding σ_u^* orbital of dioxygen. The σ_u^* of the peroxo form located at -6 eV (outside the energy window of Fig. 2) is indicated in Scheme 2, left. As the O atoms are pushed apart, the σ_u^* orbital goes down in energy, due to a decrease in the strong antibonding interactions.

To break the O–O bond of the peroxo complex, the $a_u(\sigma_u^*)$ orbital must be occupied by two more electrons, as mentioned above. As the O–O distance is increased, the antibonding interactions between the oxygen atoms are significantly decreased. Thus, the σ_u^* orbital lies at -14.5 eV when the O–O distance becomes 2.4 Å in our dioxide model, **2**. As a consequence, while in our peroxo model, **1**, the π_g^* orbitals are occupied by four electrons to create O_2^{2-}, two additional electrons are effectively transferred from the low-lying d-

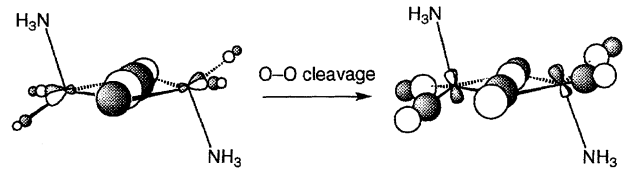

Scheme 2.

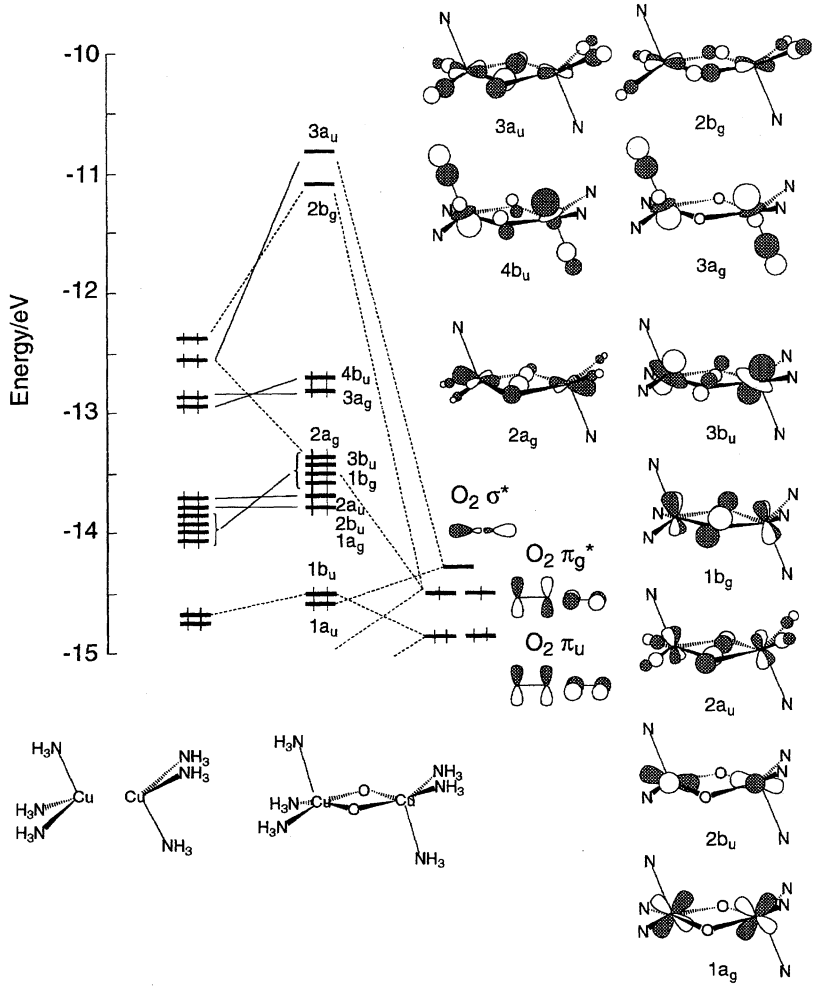

Fig. 3. Orbital interaction diagram for dicopper dioxo model complex with a (μ-O)$_2$ core structure (**2**).

block orbitals to the σ_u^* orbital to create $2O^{2-}$ in **2**. In fact, the net charge of one oxygen in the peroxo complex is −0.49, while that in the corresponding dioxo complex is −1.33.

It is essential to evaluate the activation energy for the O–O bond cleavage in order to better understand the mechanism of dioxygen activation by the dicopper enzymes. Clamer, Tolman, and their collaborators[3] did not refer to the activation energy in their recent ab initio work. We found from our qualitative calculations that the reaction should proceed with no cost of the activation energy along the O–O bond cleavage pathway. Although the extended Hückel method is not good for calculating absolute energy difference between states, the activation energy is likely to be small, even if it exists, because this reaction is symmetry allowed, judging from the profile of Fig. 2.

Let us next look at an FMO analysis for the dioxo complex **2**, shown in Fig. 3. The orbital interactions between the two oxygens are very weak in this complex; as a consequence, the bonding and antibonding levels are decreased in energy. Therefore, the σ_u^* orbital comes significantly down to cross with the copper d-block orbitals when the O–O distance becomes approximately 1.7—1.8 Å, as shown in Fig. 2. In this way, two electrons are effectively transferred from the copper d-block orbitals to the σ_u^* orbital reducing O_2^{2-} to $2O^{2-}$. Thus, almost all of the antibonding orbitals of dioxygen are filled so that the dioxygen O–O bond is reductively cleaved forming the dioxo species.

For a closer inspection of the bonding and antibonding interactions between the two oxygen atoms, we carried out MOOP (molecular orbital overlap population) analyses. Figure 4 shows such analyses for the dicopper model complexes with O–O distances of 1.4, 1.8, and 2.4 Å. The MOOP plots

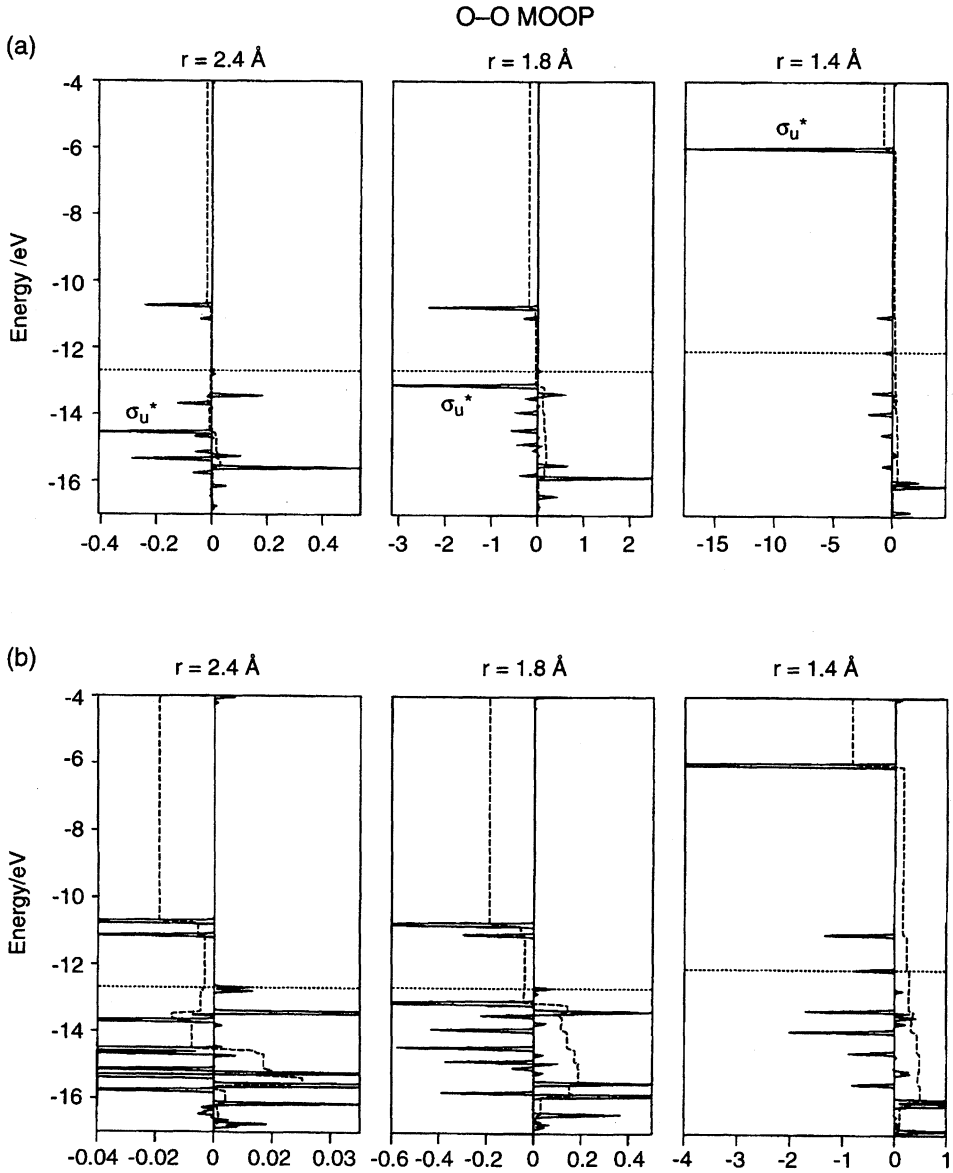

Fig. 4. (a) Molecular orbital overlap population (MOOP) curves for the O–O bond in dicopper model complexes with O–O distances (r) of 1.4, 1.8, and 2.4 Å. The dotted lines mark the HOMO levels; the dashed lines going up are the integrations of the bonding and antibonding contributions. (b) Expanded MOOP curves of (a).

for the O–O bond show the contributions of individual molecular orbitals to a Mulliken overlap population. In these, the bonding contributions are plotted to the right and the antibonding ones to the left. The dotted lines indicate the HOMO levels; the dashed lines going up are the integrations of the bonding and antibonding contributions.

It is of great use to look at the MOOP plots together with the Walsh diagram shown in Fig. 2 and the FMO analyses in Figs. 1 and 3. At an O–O distance of 1.4 Å, the HOMO is $2a_u$ (at -12.1 eV), which is slightly antibonding between the oxygen atoms, as also indicated in Fig. 1. However, $3a_u$ (at -6 eV), which is actually the antibonding σ_u^* of O_2 molecule, as indicated in Scheme 2 left, is unoccupied, so that the net integration at the HOMO level is positive, as shown in Fig. 4(b), right. This means that the peroxo species with an O–O distance of 1.4 Å has still a net bonding character although its degenerate π_g^* is fully occupied. This is consistent with a qualitative picture that the peroxo species has a bond order of 1, as mentioned above. As the O–O distance is increased, the orbital levels related to the oxygens go down; in particular, the antibonding σ_u^* orbital crosses with the HOMO level at an O–O distance of about 1.7 Å. As a result, the antibonding contribution becomes more and more dominant below the HOMO level. At an O–O distance of 1.8 Å, the net integration at the HOMO level is significantly reduced to be minus (Fig. 4(b) middle) in contrast to that at an O–O distance of 1.4 Å being plus.

We now finally look at the MOOP plot for the dioxo species with an O–O distance of 2.4 Å. The HOMO is $4b_u$ (at -12.7 eV; see Fig. 3) in which the contribution from the oxygen atoms is not significant, as indicated in Fig. 4(a), left. Most of the orbital levels related to the oxygens go down, due to a long O···O distance, and lie below the HOMO level. As a consequence, the net integration at the HOMO level is minus, as shown in Fig. 4(b), left. Therefore, the dioxo species with an O–O distance of 2.4 Å has no net O–O bonding interactions.

Conclusions

We have theoretically analyzed the electronic structures of a dicopper peroxo complex with a μ-η^2 : η^2-O_2 mode and a corresponding dioxo complex with a $(\mu\text{-O})_2$ diamond core in terms of the orbital interactions. Dioxygen O–O bond cleavage is a quite important step in the catalytic cycles of many kinds of metalloenzymes, for dioxygen activation. We thus investigated the bond cleavage on a dicopper model complex by distorting a peroxo model complex to a corresponding dioxo complex along a supposed reaction coordinate describing dioxygen O–O bond cleavage. FMO, Walsh-diagram, and MOOP analyses have shed new light on the mechanism of the electron transfer from the d-block of the metal active center to dioxygen and how the dioxygen activation occurs on a dicopper enzyme model. Qualitative calculations have shown that the activation energy for O–O bond cleavage on a dicopper model complex is likely to be small, even if it exists, because this reaction is symmetry allowed, judging from the Walsh diagram along an O–O bond cleavage pathway from **1** to **2**. We therefore think that O–O bond cleavage should proceed with no cost of the activation energy on the dicopper active site of actual enzyme systems.

This work was supported by a Grant-in-Aid for Scientific Research from the Ministry of Education, Science, and Culture. Thanks are also due to the Japan Society for the Promotion of Science (JSPS-RFTF96P00206) for its support of this work.

References

1) a) M. C. Linder and C. A. Goode, "Biochemistry of Copper," Plenum, New York (1991); b) K. D. Karlin and Z. Tyeklar, "Bioinorganic Chemistry of Copper," Chapman & Hall, New York (1993); c) J. Reedijk, "Bioinorganic Catalysis," Marcel Dekker, New York (1993); d) N. Kitajima and Y. Moro-oka, *Chem. Rev.*, **94**, 737 (1994); e) W. Kaim and B. Schwederski, "Bioinorganic Chemistry: Inorganic Elements in the Chemistry of Life," Wiley, New York (1994).

2) a) E. I. Solomon, U. M. Sundaram, and T. E. Machonkin, *Chem. Rev.*, **96**, 2563 (1996); b) E. I. Solomon, F. Tuczek, D. E. Root, and C. A. Brown, *Chem. Rev.*, **94**, 827 (1994); c) E. I. Solomon and M. D. Lowery, *Science*, **59**, 1575 (1993); d) F. Tuczek and E. I. Solomon, *Inorg. Chem.*, **32**, 2850 (1993); e) E. I. Solomon, M. J. Baldwin, and M. D. Lowery, *Chem. Rev.*, **92**, 521 (1992); f) F. Tuczek and E. I. Solomon, *Inorg. Chem.*, **31**, 944 (1992); g) P. K. Ross and E. I. Solomon, *J. Am. Chem. Soc.*, **113**, 3246 (1991); h) G. L. Woolery, L. Powers, M. Winkler, E. I. Solomon, K. Lerch, and T. G. Spiro, *Biochim. Biophys. Acta*, **788**, 155 (1984); i) R. S. Himmelwright, N. C. Eickman, C. D. Lubein, K. Lerch, and E. I. Solomon, *J. Am. Chem. Soc.*, **102**, 7339 (1980); j) N. C. Eickman, E. I. Solomon, J. A. Larrabee, T. G. Spiro, and K. Lerch, *J. Am. Chem. Soc.*, **100**, 6529 (1978).

3) a) N. Kitajima, T. Koda, S. Hashimoto, T. Kitagawa, and Y. Moro-oka, *J. Chem. Soc., Chem. Commun.*, **1988**, 151; b) N. Kitajima, K. Fujisawa, Y. Moro-oka, and K. Yoriumi, *J. Am. Chem. Soc.*, **111**, 8975 (1989); c) N. Kitajima, T. Koda, Y. Iwata, and Y. Moro-oka, *J. Am. Chem. Soc.*, **112**, 8833 (1990); d) N. Kitajima, T. Koda, S. Hashimoto, T. Kitagawa, and Y. Moro-oka, *J. Am. Chem. Soc.*, **113**, 5664 (1991); e) N. Kitajima, K. Fujisawa, and Y. Moro-oka, *Inorg. Chem.*, **29**, 357 (1990).

4) a) S. Mahapatra, J. A. Halfen, E. C. Wilkinson, G. Pan, C. J. Cramer, L. Que, Jr., and W. B. Tolman, *J. Am. Chem. Soc.*, **117**, 8865 (1995); b) J. A. Halfen, S. Mahapatra, E. C. Wilkinson, S. Kaderli, L. Que, Jr., and W. B. Tolman, *Science*, **271**, 1397 (1996).

5) C. J. Cramer, B. A. Smith, and W. B. Tolman, *J. Am. Chem. Soc.*, **118**, 11283 (1996).

6) L. Shu, J. C. Nesheim, K. Kauffmann, E. Münck, J. D. Lipscomb, and L. Que, Jr., *Science*, **275**, 515 (1997).

7) a) V. L. Pecoraro, M. J. Baldwin, and A. Gelasco, *Chem. Rev.*, **94**, 807 (1994); b) K. Sauer, V. K. Yachandra, R. D. Britt, and M. P. Klein, "Manganese Redox Enzymes," ed by V. L. Pecoraro, VCH, New York (1992); c) V. K. Yachandra, V. J. DeRose, M. J. Latimer, I. Mukerji, K. Sauer, and M. P. Klein, *Science*, **260**, 675 (1993); d) K. Wieghardt, *Angew. Chem., Int. Ed. Engl.*, **28**, 1153 (1989).

8) D. M. Proserpio, R. Hoffmann, and G. C. Dismukes, *J. Am. Chem. Soc.*, **114**, 4374 (1992).

9) R. R. Jacobson, Z. Tyeklar, A. Farooq, K. D. Karlin, S. Liu, and J. Zubieta, *J. Am. Chem. Soc.*, **110**, 3690 (1988).

10) T. Ookubo, H. Sugimoto, T. Nagayama, H. Masuda, T. Sato, K. Tanaka, Y. Maeda, H. Okawa, Y. Hayashi, A. Uehara, and M. Suzuki, *J. Am. Chem. Soc.*, **118**, 701 (1996).

11) Y. Dong, Y. Shiping, V. G. Young, Jr., and L. Que, Jr., *Angew. Chem., Int. Ed. Engl.*, **35**, 618 (1996).

12) K. Kim and S. J. Lippard, *J. Am. Chem. Soc.*, **118**, 4914 (1996).

13) K. Yoshizawa and R. Hoffmann, *Inorg. Chem.*, **35**, 2409 (1996).

14) K. Yoshizawa, T. Yamabe, and R. Hoffmann, *New J. Chem.*, **21**, 151 (1997).

15) a) B. J. Wallar and J. D. Lipscomb, *Chem. Rev.*, **96**, 2625 (1996); b) A. L. Feig and S. J. Lippard, *Chem. Rev.*, **94**, 759 (1994); c) S. J. Lippard, *Angew. Chem., Int. Ed. Engl.*, **27**, 344 (1988).

16) N. Kitajima, K. Fujisawa, C. Fujimoto, Y. Moro-oka, S. Hashimoto, T. Kitagawa, K. Toriumi, K. Tatsumi, and A. Nakamura, *J. Am. Chem. Soc.*, **114**, 1277 (1992).

17) Extended Hückel calculations were carried out using "YAeHMOP," G. Landrum, Cornell University, Ithaca, New York (1995). See: a) R. Hoffmann, *J. Chem. Phys.*, **39**, 1397 (1963); b) R. Hoffmann and W. N. Lipscomb, *J. Chem. Phys.*, **36**, 2179 (1962).

18) S. Alvarez, "Tables of Parameters for Extended Hückel Calculations," Universitat de Barcelona, Barcelona (1993).